AD-A107 820 UNIVERSITY OF SOUTHERN CALIFORNIA LOS ANGELES F/G 20/5
LASER KINETIC SPECTROSCOPIC STUDIES OF (A) THE UNIMOLECULAR REA--ETC(U)
AUG 81 R C ESTLER, H REISLER, C WITTIG N00014-80-C-0539
UNCLASSIFIED NL

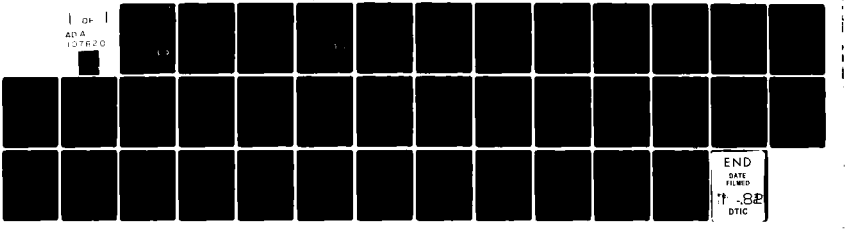

UNCLASSIFIED

SECURITY CLASSIFICATION OF THIS PAGE (When Data Entered)

LEVEL II

12

AD A107820

REPORT DOCUMENTATION PAGE	READ INSTRUCTIONS BEFORE COMPLETING FORM
1. REPORT NUMBER: N00014-80-C-0539	2. GOVT ACCESSION NO.: AD-A107820
3. RECIPIENT'S CATALOG NUMBER:	
4. TITLE (and Subtitle): LASER KINETIC SPECTROSCOPIC STUDIES OF (a) THE UNIMOLECULAR REACTIONS OF NITROALKANES AND(b) ELEMENTARY REACTIONS IMPORTANT IN COMBUSTION	5. TYPE OF REPORT & PERIOD COVERED: ANNUAL 1/1/81--8/31/81
	6. PERFORMING ORG. REPORT NUMBER:
7. AUTHOR(s): R.C. Estler, H. Reisler, C. Wittig	8. CONTRACT OR GRANT NUMBER(s): N00014-80-C-0539
9. PERFORMING ORGANIZATION NAME AND ADDRESS: UNIVERSITY OF SOUTHERN CALIFORNIA, UNIVERSITY PARK, LOS ANGELES, CA. 90007	10. PROGRAM ELEMENT, PROJECT, TASK AREA & WORK UNIT NUMBERS:
11. CONTROLLING OFFICE NAME AND ADDRESS: OFFICE OF NAVAL RESEARCH CODE 473, DEPARTMENT OF NAVY, ARLINGTON, VA. 22217	12. REPORT DATE: 10/1/81
	13. NUMBER OF PAGES: 35
14. MONITORING AGENCY NAME & ADDRESS (If different from Controlling Office)	15. SECURITY CLASS. (of this report): UNCLASSIFIED
	15a. DECLASSIFICATION/DOWNGRADING SCHEDULE:

16. DISTRIBUTION STATEMENT (of this Report)

DISTRIBUTION OF THIS DOCUMENT IS UNLIMITED

17. DISTRIBUTION STATEMENT (of the abstract entered in Block 20, if different from Report)

...ABLE.

...OF PAGES WHICH DO NOT

18. SUPPLEMENTARY NOTES

...TY.

DTIC ELECTE S NOV 30 1981 D

19. KEY WORDS (Continue on reverse side if necessary and identify by block number)

Photodissociation
Combustion
Multiphoton Ionization
Laser Photolysis
Nitrous Acid

20. ABSTRACT (Continue on reverse side if necessary and identify by block number)

(a) The multiphoton ionization (MPI) of NO is used to probe the dynamics of the photodissociation of NO_2 in a one-color experiment. The resulting MPI spectra clearly indicate the high internal rotational energy in the NO fragment. MPI shows promise as a highly sensitive, information-rich diagnostic for internal state determinations of nitric oxide. (b) We report that the 300 K reaction of C_2H with O_2 has as one of its product channels CH(~~A²Δ~~) + CO_2(~~X¹Σg⁺~~). By monitoring time resolved CH(~~A-X~~) chemiluminescence following laser photolysis production of C_2H in the presence of O_2, we have measured rate coefficients for reactions of C_2H with O_2, H_2, and CH_4.

DD FORM 1 JAN 73 1473 EDITION OF 1 NOV 65 IS OBSOLETE S/N 0102-LF-014-6601

81 11 24 004

UNCLASSIFIED

SECURITY CLASSIFICATION OF THIS PAGE (When Data Entered)

AD A107820

DTIC FILE COPY

DISCLAIMER NOTICE

THIS DOCUMENT IS BEST QUALITY PRACTICABLE. THE COPY FURNISHED TO DTIC CONTAINED A SIGNIFICANT NUMBER OF PAGES WHICH DO NOT REPRODUCE LEGIBLY.

Progress Report
January 1, 1981 to August 31, 1981

Contract No. N00014-80-C-0539

LASER KINETIC SPECTROSCOPIC STUDIES OF (a) THE UNIMOLECULAR REACTIONS OF NITROALKANES, AND (b) ELEMENTARY REACTIONS IMPORTANT IN COMBUSTION

Principal Investigators: R. C. Estler, H. Reisler, and C. Wittig

I. THE UNIMOLECULAR REACTIONS OF NITROALKANES

A. Introduction

Since the unambiguous assignment of a primary step of any decomposition process relies upon the direct observation of the primary decomposition products, we have concentrated our efforts over the past eight months in this area. For the case of the unimolecular decomposition of simple nitroalkanes (e.g., 1- and 2-nitropropane), this means direct detection of the possible primary decomposition products HONO and NO_2.

The laser induced fluorescence (LIF) spectrum of NO_2 has been well studied over the past decade and multiphoton ionization (MPI) signatures have recently been reported. In contrast, HONO is a very elusive small molecule. The inability to prepare this molecule in a pure state has, to date, limited spectroscopic studies. With the obvious interferences associated with detection by absorption and mass spectroscopy, efforts to detect HONO have focused on the techniques of LIF and MPI. Such studies are further complicated due to the photolysis of nitrous acid below 400 nm (the region of the only known electronic absorption):

$$HONO + h\nu(\lambda < 400nm) \rightarrow OH + NO \qquad (1)$$

A scheme to directly detect nitrous acid might therefore require the detection of these photodissociation fragments. Such studies are feasible using a single laser pulse as illustrated below in the study of photodissociation of NO_2. Progress in detecting HONO using these techniques is summarized below.

B. Multiphoton Ionization Detection of Photodissociation Fragments: NO from NO_2

G. Radhakrishnan, D. Ng, and R. C. Estler

The photodissociation of NO_2 to the electronic ground state species, NO and O, has been the subject of several investigations. The majority of these studies have indicated a dissociation mechanism where excess energy is distributed statistically among product degrees of freedom. Recently, Zacharias et al. have monitored the 337 nm (N_2 laser) photodissociation by one-photon LIF. They have concluded that the decay process is nonstatistical in both the rotational and vibrational degrees of freedom of product NO. Two-photon LIF has also been used successfully as a state selective probe for NO in other photodissociation studies.

We have performed a "one-color" experiment where NO_2 is first dissociated and the resulting NO is then ionized in a multiphoton transition. Both events take place within the same laser pulse (~7 nsec). The MPI spectrum of NO produced in this experiment clearly illustrates the elevated rotational temperature of the NO fragment.

In such a one-color experiment the dissociating wavelength changes as the fragment MPI spectrum is generated. In the present case, the excess energy at 382 nm is ~1050 cm^{-1} and it varies 150 cm^{-1} over the wavelength region of interest. The internal energy of NO_2 also adds to the range of excess energies available. However, in all cases, only the v = 0 level of the ground state is accessible.

The experimental apparatus consists of a biased parallel plate ion cell coupled to a nitrogen pumped dye laser. The output from the nitrogen pumped (∿10 Hz) tunable dye laser (Molectron DL14P) is focused into the ion cell by a 25 mm focal length lens. In the wavelength region of interest, dye laser pulses are ∿100 μJ and ∿7 nsec fwhm. Ion current pulses are first amplified and then synchronously detected using a boxcar integrator (PAR 162/164). The data collection and dye laser scanning are microcomputer controlled.

The preliminary results presented here are intended to illustrate the utility of the MPI technique in monitoring photodissociation dynamics. Figure 1 presents the MPI spectrum of the δ(0,0) band system of a static sample of NO, i.e.,

$$NO(X^2\Pi) \xrightarrow{2h\nu} NO(C^2\Pi) \xrightarrow{h\nu} NO^+ + e^- \qquad (2)$$

and the NO produced from the dissociation of NO_2, i.e.,

$$NO_2 \xrightarrow{h\nu} NO(X^2\Pi)+O \xrightarrow{2h\nu} NO(C^2\Pi)+O \xrightarrow{h\nu} NO^+ + e^- + O \qquad (3)$$

both at 10 mTorr and 298 K. The use of such low pressures minimizes the possibility of rotational relaxation of the nascent distribution. The spectra presented here have not been corrected for dye laser power variations (∿30% over the wavelength range of Figure 1, <10% over the wavelength region of Figure 2). The spectrum has been assigned from the absorption studies of Lagerqvist and Miescher and the two-photon absorption experiments of Freedman. The $C^2\Pi$ state is nearly Hund's case b ($A \sim 3\text{-}4\ cm^{-1}$) with a large Λ-type

doubling. The doubling, in addition to the spin-orbit split ground state, causes many of the rotational branches to overlap and makes individual line intensities difficult to determine. However, the obvious rotational excitation of the NO fragment shown in Figure 1 is easily seen by examining the region of the P_{21} band.

Figure 2 shows an expanded spectrum in the region of the $C^2\Pi - X^2\Pi$, P_{21} bandhead. The positions of the P_{21}, Q_{21}, and Q_{11} branch lines are indicated. Most of the peaks in the MPI spectrum consist of two or three overlapping lines. However, some of the Λ-doublet components of the P_{21} branch are resolvable. In comparing the room temperature NO spectrum with respect to the "fragment" NO spectrum, it is these high rotational P_{21} lines which grow in intensity with respect to the lower rotational lines of the Q_{21} branch. Assuming the ion signals are proportional to the square of the laser power and a two-photon transition line strength, the intensities of the P_{21} branch can be used to obtain an estimate of the rotational excitation of the NO photodissociation fragment. Using the resolvable Λ-doublet components of this branch (for J = 12.5 to 18.5), we obtain a rotational population distribution that is well described by a temperature of 1500 K. This compares to 1600 K for high rotational levels of several vibrational states measured by Zacharias et al. To check the validity of our calculated two-photon line strengths, a similar analysis was performed on the room temperature spectrum. A rotational temperature of 310 K is

indicated verifying the analysis procedure. Clearly, however, accurate determination of such distributions awaits more detailed analysis and modelling of the MPI signal intensities. Yet, the basis for using MPI as an internal state probe for nitric oxide is clearly demonstrated.

Various excess energies may be investigated using this one-color technique by tuning the laser to other two-photon resonances of NO where one photon is to the blue of the NO_2 dissociation threshold, e.g., the $\delta(1,0)$ band system. These studies are currently underway in our laboratory.

Acknowledgment

We are grateful to the Office of Naval Research for support of this research. We are also indebted to Professor Ernst Miescher for his enlightening correspondence.

REFERENCES

1. G.E. Busch and K.R. Wilson, J. Chem. Phys. 56 (1972) 3626.

2. G.E. Busch and K.R. Wilson, J. Chem. Phys. 56 (1972) 3638.

3. M. Quack and J. Troe, Ber. Buns. Ges. Phys. Chem. 79 (1975) 469.

4. H. Gaedtke and J. Troe, Z. Naturforsch. Teil A 25 (1970) 789.

5. H. Zacharias, M. Geilhaupt, K. Meier, and K.H. Welge, J. Chem. Phys. 74 (1981) 218.

6. M. Asscher, Y. Haas, M.P. Roellig, and P.L. Houston, J. Chem. Phys. 72 (1980) 768; 73 (1980) 5081.

7. T.E. Adams, R.J.S. Morrison, and E.R. Grant, Rev. Sci. Instrum. 51 (1980) 141.

8. R.C. Estler, Rev. Sci. Instrum. 51 (1980) 1428.

9. A. Lagerqvist and E. Miescher, Helv. Phys. Acta 31 (1958) 221.

10. P.A. Freedman, Can. J. Phys. 55 (1977) 1387.

11. R. G. Bray and R. M. Hochstrasser, Mole. Phys. 31 (1976) 412.

FIGURE CAPTIONS

Fig. 1 Multiphoton ionization spectra of $\delta(0,0)$ band system of NO: A) pure NO at 10 mtorr, 298 K and, B) NO from photodissociated NO_2 at 10 mTorr, 298 K. Prominent bandhead positions are indicated. Spectrum B has been displaced slightly from spectrum A for clarity.

Fig. 2 Multiphoton ionization spectra of NO in the region of the $\delta(0,0)$ P_{21} and Q_{21} bandhead positions: A) pure NO at 10 mTorr and 298 K and B) NO from photodissociated NO_2 at 10 mTorr, are indicated. The numbers adjacent to the line positions are J-1/2. The spectra have been normalized in such a manner to make the P_{11} bandhead (not shown) the same intensity in both spectra.

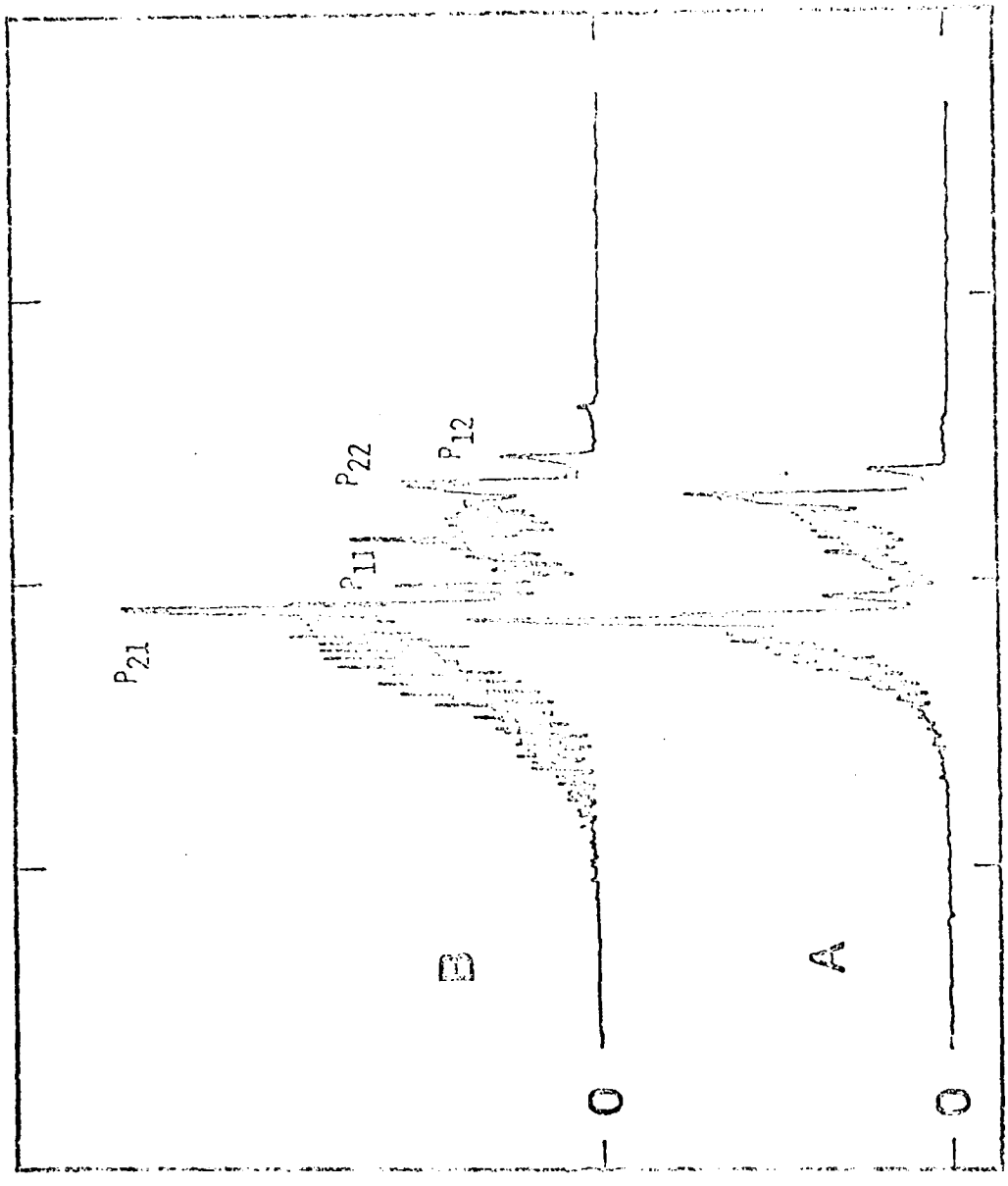
P21
P111
P22
P12
B
A
0
0
880
882
884
Wavelength (nm)
ion intensity

FIGURE 1

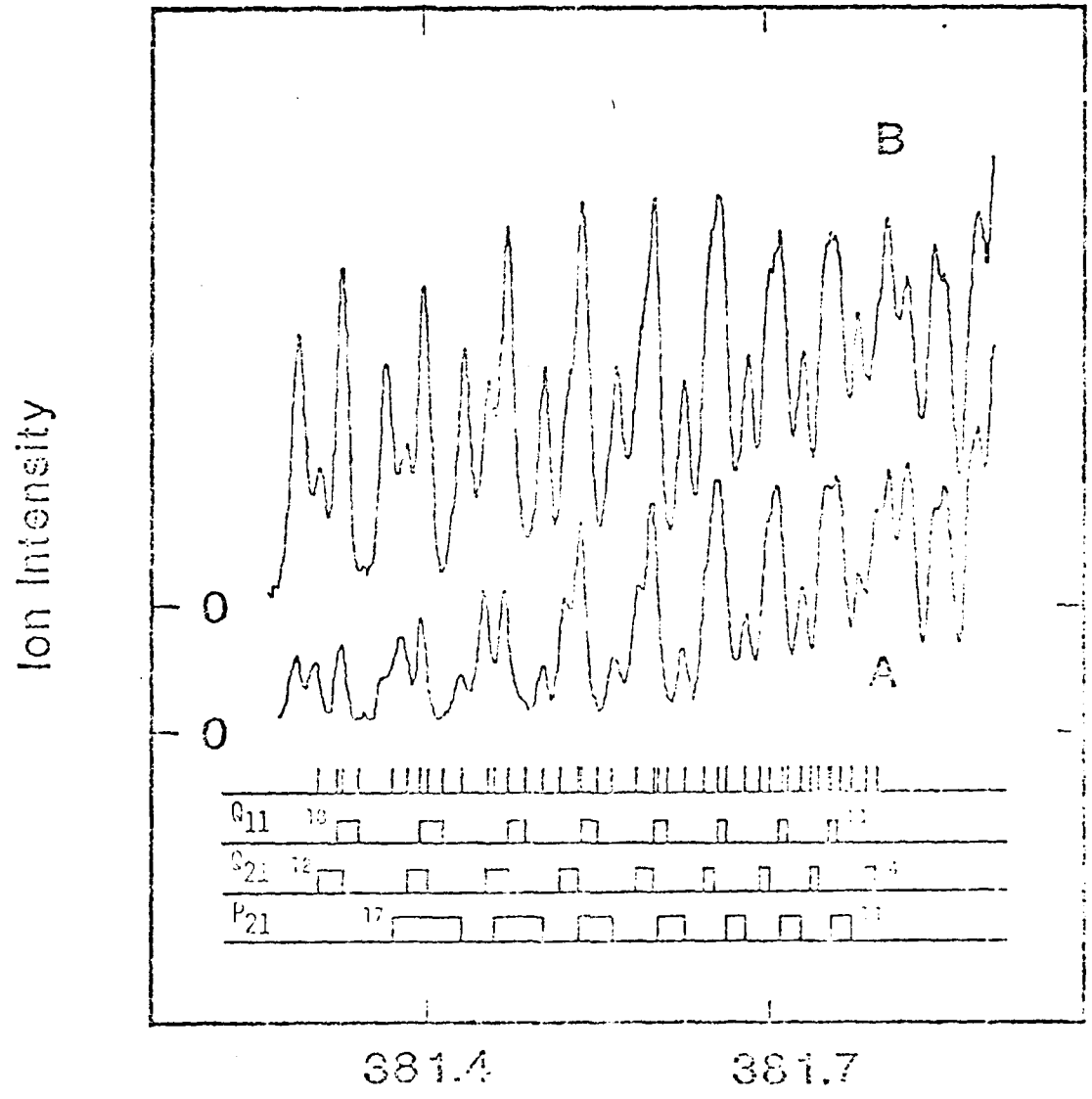

FIGURE 2.

C. Detection of NO from HONO

In a single laser experiment identical to that described in Section B, we attempted to detect HONO via MPI detection of NO resulting from the photodissociation of nitrous acid (equation 1, Section A). Even though there may be other sources of NO present (e.g., $NO_2 \xrightarrow{h\nu} NO + O$), unambiguous detection of HONO is still possible if the internal state distribution of the resulting NO fragment is different from other sources.

Experiments were performed using equilibrium mixtures:

$$NO + NO_2 + H_2O \rightleftarrows 2HONO \qquad (4)$$

Multiphoton ionization spectra of NO were recorded as described previously, but showed no new rotational structure (i.e., different from that recorded from either NO or NO_2).

Similar experiments using one- or two-photon LIF of NO for HONO detection would certainly suffer from the same spectroscopic contamination problems. Other sources of NO (particularly using equilibrium mixtures) will mask the NO resulting from the nitrous acid photolysis. For these reasons detection of NO signatures following photodissociation has been abandoned as a detection scheme for HONO.

D. Detection of OH from HONO

Unlike nitric oxide, the hydroxyl radical (the second product of the nitrous acid photolysis) should have a single precursor, thereby eliminating any masking effects.

There have been numerous studies of the one-photon LIF of OH, particularly in the region of the $A^2\Sigma^+(v' = 0) \leftarrow X^2\Pi(v'' = 0)$ transition, ~309 nm. Since this transition occurs below the threshold of the HONO photolysis, it is an excellent candidate for single frequency laser detection.

The experimental arrangement used for these studies is similar to that used in the MPI studies. A flow cell is maintained at a given pressure with sample. The output of a doubled nitrogen-pumped dye laser passes through the cell crossing a viewing window. The fluorescence is imaged onto the face of a photomultiplier tube by a field-stop limited telescope.[1,2] Photomultiplier tube pulses are processed identically to MPI pulses (boxcar integration under microcomputer control).

Using two sources for nitrous acid, equilibrium mixtures and a chemical generator,[3] we have observed extremely weak fluorescence signals in the region of the A-X OH transitions. Since these signals are on the same order of magnitude as the experimental noise, further studies are necessary prior to conclusively assigning these signals to hydroxyl radical. One reason for the weak signals is the low output power of the dye laser doubling system. Since this output is used for both dissociation and induced fluorescence, its intensity is a

critical parameter.

Two experiments are currently underway in our laboratory to improve the signal-to-noise ratios observed so as to prove/disprove OH detection from photodissociated HONO. First, simply focusing the UV beam with the cell will increase the intensity and thereby the probability of dissociation and induced fluorescence occurring within the laser pulse. A second procedure currently being implemented uses part (~25%) of the pumping nitrogen laser pulse to dissociate the nitrous acid. This procedure insures a high probability of dissociation. The probing beam is delayed from the dissociating pulse a few nanoseconds due to optical path differences.

References

1. C. K. Man and R. C. Estler, J. Chem. Phys. 75, 2779 (1981).

2. R. E. Smalley, D. A. Auerbach, P. S. H. Fitch, D. H. Levy, and L. Wharton, J. Chem. Phys. 66, 3778 (1977).

3. G. E. Streit, J. S. Wells, F. C. Fehsenfeld, and C. J. Howard, J. Chem. Phys. 70, 3439 (1979).

E. Pyrolysis Source

The pyrolysis source that will be used for the nitroalkane decomposition studies is nearing completion and will undergo tests shortly. The source is similar to the design of the high temperature oven of Dagdigian and Wharton.[1] A quartz reactor is surrounded by a thin-walled (0.25 - 0.5mm) stainless steel tube and radiantly heated up to 1200°K by passing a large alternating current (300 A) through this surrounding heater tube. A water-cooled copper jacket encloses the entire oven assembly. Residence times within the reaction can be controlled by flow rate and/or length of reactor heated.

---

[1] P. J. Dagdigian and L. Warton, J. Chem. Phys. 57, 1487 (1972).

II. GAS PHASE REACTIONS OF $C_2H(\tilde{X}^2\Sigma^+)$ WITH O_2, H_2, AND CH_4 STUDIED VIA TIME RESOLVED PRODUCT EMISSIONS

A. M. Renlund, F. Shokoohi, H. Reisler, and C. Wittig

ABSTRACT

We report that the 300 K reaction of C_2H with O_2 has as one of its product channels $CH(\underline{A}^2\Delta) + CO_2(\tilde{X}^1\Sigma_g^+)$. By monitoring time resolved $CH(\underline{A}-\underline{X})$ chemiluminescence following laser photolysis production of C_2H in the presence of O_2, we have measured rate coefficients for reactions of C_2H with O_2, H_2, and CH_4.

I. INTRODUCTION

The precise identification of the chemical and physical processes which are germane to the oxidation of hydrocarbon fuels is an arduous task, and for even the least complex systems a myriad of pathways must be sorted out if our understanding is to be predictive. Experimental research has been instrumental in providing a data base with which calculations can be compared, albeit not as rapidly as many enthusiasts had hoped. In this communication, we present measurements of rate coefficients for the reactions of the ethynyl radical, C_2H, with O_2, H_2, and CH_4. This is part of an ongoing research effort in which elementary kinetic processes of small carbonaceous gas phase free radicals are studied by laser kinetic spectroscopy,[1] in order to understand certain combustion processes in as much detail as possible.

C_2H is an extremely important species in combustion environments, as it contributes to soot formation,[2] and can undergo a number of interesting reactions with hydrocarbons. C_2H is also abundant in interstellar space.[3] The most detailed spectroscopic information derives from ESR measurements on C_2H trapped in a 4 K Ar matrix.[4] Measurements of ir spectra have resulted in tentative assignments,[5,6] but to date no electronic states of C_2H have been positively identified.[4] Despite its importance, only a few measurements of absolute rate coefficients and of reactions with oxidizing agents have been reported,[7,8] in part due to the lack of a suitable means by which C_2H can be prepared and monitored in well controlled environments.

In separate experiments, we have searched, with high sensi-

I. INTRODUCTION

The precise identification of the chemical and physical processes which are germane to the oxidation of hydrocarbon fuels is an arduous task, and for even the least complex systems a myriad of pathways must be sorted out if our understanding is to be predictive. Experimental research has been instrumental in providing a data base with which calculations can be compared, albeit not as rapidly as many enthusiasts had hoped. In this communication, we present measurements of rate coefficients for the reactions of the ethynyl radical, C_2H, with O_2, H_2, and CH_4. This is part of an ongoing research effort in which elementary kinetic processes of small carbonaceous gas phase free radicals are studied by laser kinetic spectroscopy,[1] in order to understand certain combustion processes in as much detail as possible.

C_2H is an extremely important species in combustion environments, as it contributes to soot formation,[2] and can undergo a number of interesting reactions with hydrocarbons. C_2H is also abundant in interstellar space.[3] The most detailed spectroscopic information derives from ESR measurements on C_2H trapped in a 4 K Ar matrix.[4] Measurements of ir spectra have resulted in tentative assignments,[5,6] but to date no electronic states of C_2H have been positively identified.[4] Despite its importance, only a few measurements of absolute rate coefficients and of reactions with oxidizing agents have been reported,[7,8] in part due to the lack of a suitable means by which C_2H can be prepared and monitored in well controlled environments.

In separate experiments, we have searched, with high sensi-

tivity, for C_2H absorptions in the region 220 - 700 nm, and found none. This was done by photolyzing C_2H precursors at 193 nm, while measuring absorption spectra with a standard "probe flash" and grating spectrometer. Having found no absorptions, we proceeded to investigate in greater detail the $CH(A^2\Delta-X^2\Pi)$ chemiluminescence observed previously in our laboratory following ir multiple photon dissociation (MPD) of C_2H_3CN and several alkenes in the presence of O_2.[9] It was suggested that the reaction:

$$C_2H(\tilde{X}^2\Sigma^+) + O_2(X^3\Sigma_g^-) \xrightarrow{k_1} CH(A^2\Delta) + CO_2(\tilde{X}^1\Sigma_g^+) \qquad (1)$$

$$\Delta H^\circ = -144.1 \text{ kcal mol}^{-1}$$

may be responsible for the $CH(A^2\Delta-X^2\Pi)$ chemiluminescence, but this was not the main focus of these earlier experiments, and no effort was made to resolve the issue at that time.

As a general practice, it is undesirable to study reaction kinetics by monitoring only product emissions. Clearly, it is most desirable to monitor spectroscopically the removal of the reactant species of concern. In the case of C_2H, where there is no absorption in the region 220 - 700 nm, our inability to spectroscopically monitor this species directly has caused us to go to great lengths to insure that species other than C_2H do not play a role in our experiments.

Observation of time resolved $CH(A^2\Delta-X^2\Pi)$ chemiluminescence from reaction (1) allows us to determine rate coefficients for the removal of $C_2H(\tilde{X}^2\Sigma^+)$ by a variety of species. Here, we report rate coefficients for C_2H removal by O_2, H_2 and CH_4. These reactants are representative of larger classes of species which are currently being studied in our laboratory and will be reported in subsequent publications.

II. EXPERIMENTAL

In the present experiments, we rely on the time resolved detection of chemiluminescent products in order to monitor reaction. C_2H precursors are photodissociated in a fluorescence chamber using either the unfocused output from an ArF excimer laser at 193 nm (Lumonics, TE 261-2 or TE 861S-2) or the focused output from a CO_2 TEA laser (Tachisto 215G). $CH(A-X)$ chemiluminescence is detected at right angles to the photolysis beam with a photomultiplier tube (PMT) whose output is processed by a transient digitizer/signal averager combination with a minimum gate width of 10 ns. In time resolved measurements, a narrow bandpass interference filter centered at 432.6 nm (7 nm fwhm) is used to isolate the $CH(A-X)$ emission. Typically, results from 16-64 laser firings are averaged for each datum. Chemiluminescence spectra are obtained using a 0.25 m Jarrell-Ash monochromator. The spectra are obtained point-by-point (0.2 nm increments, 0.4 nm resolution) and time integrated signals from 64 laser firings are averaged at each wavelength setting.

CO_2 ir chemiluminescence ($\Delta v_3=1$) is monitored at right angles to the photolysis beam with an InSb detector (Spectronics, photovoltaic, 77 K, 1.2 cm^2). A narrow bandpass interference filter centered at 2300 cm^{-1} (120 cm^{-1} fwhm) is used to isolate a part of the CO_2 $\Delta v_3=1$ emission. Signals from the detector are amplified and processed with the transient digitizer/signal averager combination. Typically, results from 64 laser firings are averaged for each datum.

The measured rate coefficients should not depend on the C_2H precursor, and to insure that this is true, we have used a number

of different precursor molecules in our experiments. C_2H_2, C_2HBr, and C_2HCHO were all dissociated with the unfocused 193 nm output from the ArF laser (<25 mJ cm^{-2}). C_2HCHO was also dissociated with the focused output from the CO_2 TEA laser tuned to the (001)-(100) P(10) transition at 953 cm^{-1}, which overlaps the maximum in the R-branch of the ν_6 (C-C stretch) vibration of C_2HCHO.[10]

C_2HBr was prepared by dehydrobromination of 1,2-dibromoethylene as per ref. 11; C_2HCHO was prepared as per ref. 12. Both of these, as well as C_2H_2 (Airco), were purified by repeated trap-to-trap distillations. Sample purities were confirmed by comparing their ir spectra to published spectra.[13] Samples were subjected to freeze-pump-thaw cycles just prior to use. O_2(99.99%), Ar(99.998%), He(99.999%), H_2(99.99%), and CH_4(99.99%) were used without further purification.

In a typical experiment, a premixed sample containing the C_2H precursor, O_2, and Ar or He diluent is passed slowly through the fluorescence chamber. Sufficient O_2 is present to insure sensibly first order kinetics. Constituent pressures are typically 1-6 mTorr of the C_2H precursor, 20 - 400 mTorr O_2, and Ar or He added to give total pressures of 200 - 800 mTorr. Observation times for the CH(A-X) signals are typically 15 - 30 μs, while under the experimental conditions wherein CO_2 Δv_3=1 emission is monitored, the emission persists for ~1 ms, with signal risetimes of 25 - 100 μs.

III. RESULTS

Chemiluminescence spectra

Since we are monitoring reactions via chemiluminescence, it is imperative that we establish unambiguously the identity of the emitting species. Figure 1 shows a spectrum obtained when C_2H_2 is dissociated in the presence of O_2. It corresponds to the well known A-X emission spectrum of CH,[12] showing vibrational excitation to $v'=2$. The 0,0 and 1,1 bands overlap each other and are not resolved in our spectrum. The broad features appearing at 433 - 436 nm are due to contributions from the Q-branch heads of the 2,2 band, as well as from P-branch lines of the vibrational band systems. Emission to the short wavelength side of the main peak is due to high rotational levels of the 0,0 and 1,1 bands. Such clearly identifiable CH(A-X) emission spectra were obtained for all C_2H precursor molecules used in our experiments. We defer to a future publication any detailed analyses of the spectra. Here we are primarily concerned with the positive identification of the emission which we will use to monitor the reaction.

Reaction kinetics

Reaction (1) is but a single channel of the overall reaction of C_2H with O_2:

$$C_2H(\tilde{X}^2\Sigma^+) + O_2(X^3\Sigma_g^-) \xrightarrow{k_2} \text{products} \qquad (2)$$

Product channels other than reaction (1) will be the subject of our future research. In the present experiments, reaction (1) is used in order to monitor C_2H removal, thereby allowing us to

measure rate coefficients for the overall reactions of C_2H with added species.

A typical time resolved $CH(A-X)$ emission signal is shown in fig. 2. The decay portion is easily fit to a single exponential, from which reaction rate coefficients for the total removal of C_2H are obtained by the usual systematic variations of reagent concentrations. The largest signals were obtained when C_2HCHO was dissociated at 193 nm in the presence of O_2. Dissociation of C_2HCHO with the focused output from the CO_2 laser gave ~ two orders of magnitude less signal.

The solution of the rate equations pertaining to $CH(A-X)$ chemiluminescence is straightforward, and for the case of the reaction of C_2H with O_2 yields:

$$I(t) = \frac{k_1[O_2][C_2H]_0}{(\tau_{rad}^{-1}+\tau_{Q,D}^{-1})-(k_2[O_2]+k_p[\text{precursor}])} \times$$

$$\times \{\exp\{-(k_2[O_2]+k_p[\text{precursor}])t\}-\exp\{-(\tau_{rad}^{-1}+\tau_{Q,D}^{-1})t\} \quad (2)$$

where $[C_2H]_0$ is the initial C_2H concentration, k_p is the rate coefficient for the reaction of C_2H with its precursor, τ_{rad}^{-1} is the $CH(A-X)$ radiative rate = 1.9×10^6 s^{-1},[13] and $\tau_{Q,D}^{-1}$ is the combined rate of quenching and diffusion of $CH(A)$. The first exponential term in the brackets represents the decay portion of the time resolved emission. Thus, k_2 is obtained from a plot of the signal decay rate versus $[O_2]$, and such data are shown in fig. 3. It is clear from fig. 3 that k_2 is the same for the various C_2H precursors.

It is also possible to determine k_2 by monitoring CO_2 ir

chemiluminescence. Here, because of the long spontaneous emission lifetime, the rate of reaction is manifest in the rise, rather than the fall, of the chemiluminescence signal, in contrast to the case of $CH(A)$. The fall of the signal reflects all processes which remove CO_2^* (spontaneous emission, diffusion, and collisional deexcitation). Since the rise and the fall times are not as different as in the case of $CH(A)$ emission, it is necessary to carefully deconvolute the CO_2^* signals in order to obtain reaction rates.[16] The rates thus extracted, although inherently less accurate than those obtained from the $CH(A)$ emissions, are nevertheless in good agreement with those obtained using the $CH(A-X)$ emissions. Table I summarizes all of the $C_2H + O_2$ rate coefficient measurements; the average value of k_2 is $(2.1\pm0.3)\times10^{-11}$ cm^3 $molec^{-1}$ s^{-1}, in good agreement with our previous estimate.[9]

When adding other reactants to the gas sample, the rate of reaction becomes $k_2[O_2] + k_p[precursor] + k_i[M_i]$, where k_i is the rate coefficient for the added reactant M_i. Thus, k_i is obtained from a plot of the $CH(A-X)$ signal decay rate *vs* $[M_i]$, as described above. Results for H_2 and CH_4 are shown in fig. 4, and the k_i thus obtained are $(1.2\pm0.3)\times10^{-11}$ and $(4.8\pm1.0)\times10^{-11}$ cm^3 $molec^{-1}$ s^{-1} for H_2 and CH_4, respectively.

IV. DISCUSSION

It is a bit frustrating to be unable to monitor C_2H optically, since its isoelectronic counterpart, CN, is particularly amenable to optical detection via the $B^2\Sigma^+ - X^2\Sigma^+$ system in the uv.[17] The analogous vertical transition in C_2H, the excitation of a 4σ electron to the 5σ orbital, is calculated to be in excess of 7 eV since it involves the excitation of a CH σ-bonding electron.[18,19] Despite the inability to "see" C_2H, our experiments clearly indicate that the reaction of C_2H with O_2 is responsible for the $CH(A^2\Delta)$ and CO_2 ($\Delta v_3=1$) emissions. C_2H is a known photoproduct in the uv dissociation of C_2HBr trapped in an Ar matrix, where it has been identified by its ESR spectrum.[4] Similarly, uv dissociation of the other precursor molecules should yield C_2H. Also, the precursors which we have dissociated by the MFD are known to lead to C_2 under collisionless conditions,[20,23] and for most of the alkenes and for C_2HCHO, a likely precursor to C_2 is C_2H. No other nascent photofragments can participate in sufficiently exoergic reactions to account for the production of $CH(A^2\Delta)$. Mechanisms invoking reactions between two photofragments are inconsistent with the data shown in figs. 3 and 4, and consecutive reactions can likewise be eliminated (e.g., by inspection of the rise of the $CH(A^2\Delta)$ signals). The fact that both $CH(A^2\Delta)$ and CO_2^+ appear with the same rate indicates that they are products of the same reaction. We are aware that uv dissociation using excimer lasers may, under certain conditions, be quite severe, and $CH(A^2\Delta)$ has been observed as a nascent photoproduct in the dissociation of C_2H_2 as a two-photon product even using an unfocused ArF laser.[22] We checked for the possibility

of this and other two-photon processes (e.g., by looking for C_2 via LIF) and saw no evidence of such processes at the low fluences employed here. The only additional species worth consideration is the $A^2\Pi$ state of C_2H which has been calculated to be at fairly low energy, but still separated by >20 kcal mol^{-1} from the ground state.[18,19] While this state may be formed in the uv photolysis of the precursor molecules, it is highly unlikely that it would be accessed via IR MPD photolysis. We therefore feel justified in neglecting this species as a significant contributor in the observed reactions.

The reaction of C_2H with O_2 may begin with the overlap of the C_2H unpaired σ electron and an unpaired π electron centered on either oxygen atom. This would be followed by rearrangements to the different transition states. Being a peroxy radical, the O_2C_2H complex can have a reasonable lifetime and the associated depression in the multidimensional potential energy surface may facilitate the rearrangements required for different product channels. In this regard, measurements of other exothermic product channels (e.g., CO + CHO, C_2O + OH, CH($\underline{X}$) + CO_2) will be most illuminating. We are currently studying the various product channels in more detail, and further discussion of the mechanism of the $C_2H + O_2$ reaction will be presented in a later publication.

We concentrate here on a discussion of the rates of the reactions which we measured. Very little is known about the reactivity of C_2H, although <u>relative</u> rates for reaction with various hydrocarbons have been reported,[23,24]. The only other absolute rate coefficients of which we are aware have been

measured by Lange and Wagner[7] for H_2, O_2 and C_2H_2, and by Laufer and Bass[8] for H_2 and C_2H_2. Both of those studies employed detection techniques which are not particularly suited for monitoring fast reactions. They obtained rate coefficients which are slower than those which we have measured, but because our time resolution allows us to obtain reliable data at very short times (see fig. 2), we feel our experimental technique is more suitable for studying fast reactions. Clearly, C_2H is a highly reactive species and is an important constituent in combustion processes. For example, the $CH(A-X)$ emission which is characteristic of C_2H_2/O_2 flames,[25] and is thought to derive from the reaction of C_2 with OH, may be due in large part to the reaction of C_2H with O_2.

The earlier studies of C_2H,[23,24] which relied on the classical techniques of product analysis and radical scavengers, indicate that C_2H reacts with alkenes by H-atom abstraction. Reaction pathways for C_2H with H_2 and CH_4 are thus:

$$C_2H(\tilde{X}^2\Sigma^+) + H_2(X^1\Sigma_g^+) \longrightarrow C_2H_2(\tilde{X}^1\Sigma_g^+) + H(^2S_g) \qquad (4)$$
$$\Delta H^\circ \approx -21 \text{ kcal mol}^{-1}$$

$$C_2H(\tilde{X}^2\Sigma^+) + CH_4(\tilde{X}^1A_1) \longrightarrow C_2H_2(\tilde{X}^1\Sigma_g^+) + CH_3(\tilde{X}^2A_2'') \qquad (5)$$
$$\Delta H^\circ \approx -21 \text{ kcal mol}^{-1}$$

Both reactions are exothermic and allowed by state correlation. Since C_2H is a σ- free radical, it should readily accept transfer of an H-atom 1s electron. This is indeed indicated by the fast reaction rates measured. For example, C_2H is more reactive than

$C_2(X^1\Sigma_g^+)$ which is a closed shell species.[26] C_2H is also significantly more reactive than $C_2(a^3\Pi_u)$ which is apparently nonreactive with H_2, and reacts only slowly ($k<10^{-16}$ cm^3 molec^{-1} s^{-1}) with CH_4.[27]

The results we have presented here comprise only preliminary investigations, and studies of C_2H reactions may now proceed in several directions. We have recently extended our experiments to include additional C_2H sources, (e.g., CF_3C_2H) and we have also identified at least one other pathway for reaction (1): the formation of $CO(a'^3\Sigma^+)$ at a rate which is in agreement with those presented here. We feel these recent results further strengthen the arguments presented here in identifying C_2H as the reactant species, and the results of these experiments will be presented in future publications. Also, using reaction (1), it will be straightforward to determine reaction rate coefficients for several species of interest in combustion. This is particularly necessary since these preliminary results show C_2H to be very reactive. Detailed studies of product branching ratios and of reaction mechanisms should also prove very illuminating, and such experiments are currently being pursued in our laboratory.

ACKNOWLEDGEMENTS

We gratefully acknowledge helpful discussions with S.V. Filseth, G. Herzberg and J.J. Tiee. We also thank D. Dows for the loan of equipment.

REFERENCES

1. For a recent review, see: H. Reisler, M.S. Mangir, and C. Wittig, in: Chemical and Biochemical Applications of Lasers, Vol. 5, ed. C.B. Moore (Academic Press, New York, 1980) p. 139.

2. K.H. Homann and H.G. Wagner, Proc. R. Soc. Lond. A 307 (1967) 141.

3. K.D. Tucker, M.L. Kutner and P. Thaddeus, Astrophys. J. 193 (1974) L115.

4. W.R.M. Graham, K.I. Dismuke and W. Weltner, Jr., a) J. Chem. Phys. 60 (1974) 3817, b) J. Chem. Phys. 63 (1975) 2264.

5. D.E. Milligan, M.E. Jacox and L. Abouaf-Marguin, J. Chem. Phys. 46 (1967) 4562.

6. M.E. Jacox, Chem. Phys. 7 (1975) 424.

7. W. Lange and H. Gg. Wagner, Ber. Bunsenges. Phys. Chem. 79 (1975) 165.

8. A.H. Laufer and A.M. Bass, J. Phys. Chem. 83 (1979) 310.

9. H. Reisler, M. Mangir and C. Wittig, Chem. Phys. 47 (1980) 49.

10. J.C.D. Brand and J.K.G. Watson, Trans. Faraday Soc. 56 (1960) 1582.

11. L.A. Bashford, H.J. Emelius and H.V.A Briscoe, J. Chem Soc. (Lond) II (1938) 1358.

12. V.F. Wille, L. Saffer and V.W. Weisskopf, Liebigs Ann. Chem. 568 (1950) 34.

13. For C_2HBr, see: K. Evans, R. Schops, S. Rice and D. Heller, J.C.S. Faraday II 69 (1973) 858. For C_2HCHO, see ref. 8. For C_2H_2, see: T. Shimanouchi, Tables of Molecular Vibrational Frequencies, Consolidated Vol. 1, NSRDS-NBS 39 (1972).

14. A.M. Bass and H.P. Broida, NBSM 24 (1961).

15. J. Brzozowski, P. Bunker, N. Elander and P. Erman, Astrophys J. 207 (1976) 414.

16. See, e.g., A. Hariri and C. Wittig, J. Chem. Phys. 67 (1977) 4454, and H. Reisler and C. Wittig, J. Chem. Phys. 69 (1978) 3729.

17. G. Herzberg, Molecular Spectra and Molecular Structure, Vol. 1, Spectra of Diatomic Molecules (Van Nostrand, Princeton, 1950).

18. S. Shih, S.D. Peyerimhoff and R.J. Buenker, J. Mol. Spectry. 64 (1977) 167.

19. V. Staemmler, unpublished.

20. N.V. Chekalin, V.S. Letokhov, V.N. Lokhman and A.N. Shibanov, Chem. Phys. 36 (1979) 415.

21. M.L. Lesiecki, G.R. Smith, J.A. Stewart and W.A. Guillory, Chem. Phys. 46 (1980) 321.

22. W.M. Jackson, J.B. Halpern and C.S. Lin, Chem. Phys. Letters 55 (1978) 254.

23. A.M. Tarr, O.P. Strausz and H.E. Gunning, Trans. Faraday Soc. 61 (1965) 1946.

24. C.F. Cullis, D.J. Hucknall and J.V. Shepherd, Proc. R. Soc. Lond. A 335 (1973) 525.

25. A.G. Gaydon, The Spectroscopy of Flames (Wiley, New York, 1957).

26. L. Pasternack and J.R. McDonald, Chem. Phys. 43 (1979) 173.

27. V.M. Donnelly and L. Pasternack, Chem. Phys. 39 (1979) 427.

TABLE I

Precursors and emissions used in measuring the rate coefficient, k_2, for the reaction of $C_2H(\tilde{X}^2\Sigma^+)$ with $O_2(\tilde{X}^3\Sigma_g^-)$.

precursor	photolysis source	emission monitored	k_2 (units of $10^{-11}cm^3molec^{-1}s^{-1}$)
C_2H_2	193 nm	$CH(A-X)$	2.0±0.3
	193 nm	$CO_2(\Delta v_3=1)$	1.8±0.5
C_2HBr	193 nm	$CH(A-X)$	2.2±0.3
C_2HCHO	193 nm	$CH(A-X)$	2.1±0.2
	193 nm	$CO_2(\Delta v_3=1)$	1.9±0.4
	ir MPD	$CH(A-X)$	2.2±0.5
C_2H_3CN[a]	ir MPD	$CH(A-X)$	2.5±0.2

[a]from ref. 9. C_2H is formed via sequential photolyses; the immediate precursor is C_2HCN.

FIGURE CAPTIONS

Fig. 1. $CH(A^2\Delta \rightarrow X^2\Pi)$ chemiluminescence spectrum that results from the reaction of C_2H with O_2. This spectrum was taken with 60 mTorr C_2H_2 and 540 mTorr O_2, photolyzed at 193 nm. The monochromator was scanned in 0.2 nm steps with 0.4 nm resolution.

Fig. 2. Time resolved CH(A-X) chemiluminescence signal following 193 nm laser photolysis of 6 mTorr C_2H_2 in the presence of 300 mTorr O_2 and 300 mTorr He. Fluorescence was observed through an interference filter centered at 432.6 nm. The curve was obtained by averaging results from 32 laser firings. The initial spike is due to window fluorescence.

Fig. 3. The decay rate of CH(A-X) emission from reaction (1) vs O_2 pressure. C_2H was generated by : ○ C_2HCHO photolysis at 193 nm; △ C_2H_2 photolysis at 193 nm; □ C_2HBr photolysis at 193 nm; ○ C_2HCHO dissociated by ir MPD.

Fig. 4. The decay rate of CH(A-X) emission from reaction (1) vs pressure of added reagents: ○ H_2, △ CH_4. C_2H was generated by photolysis of C_2H_2 at 193 nm. The intercepts include contributions due to quenching, diffusion, reaction with O_2, and radiative decay.

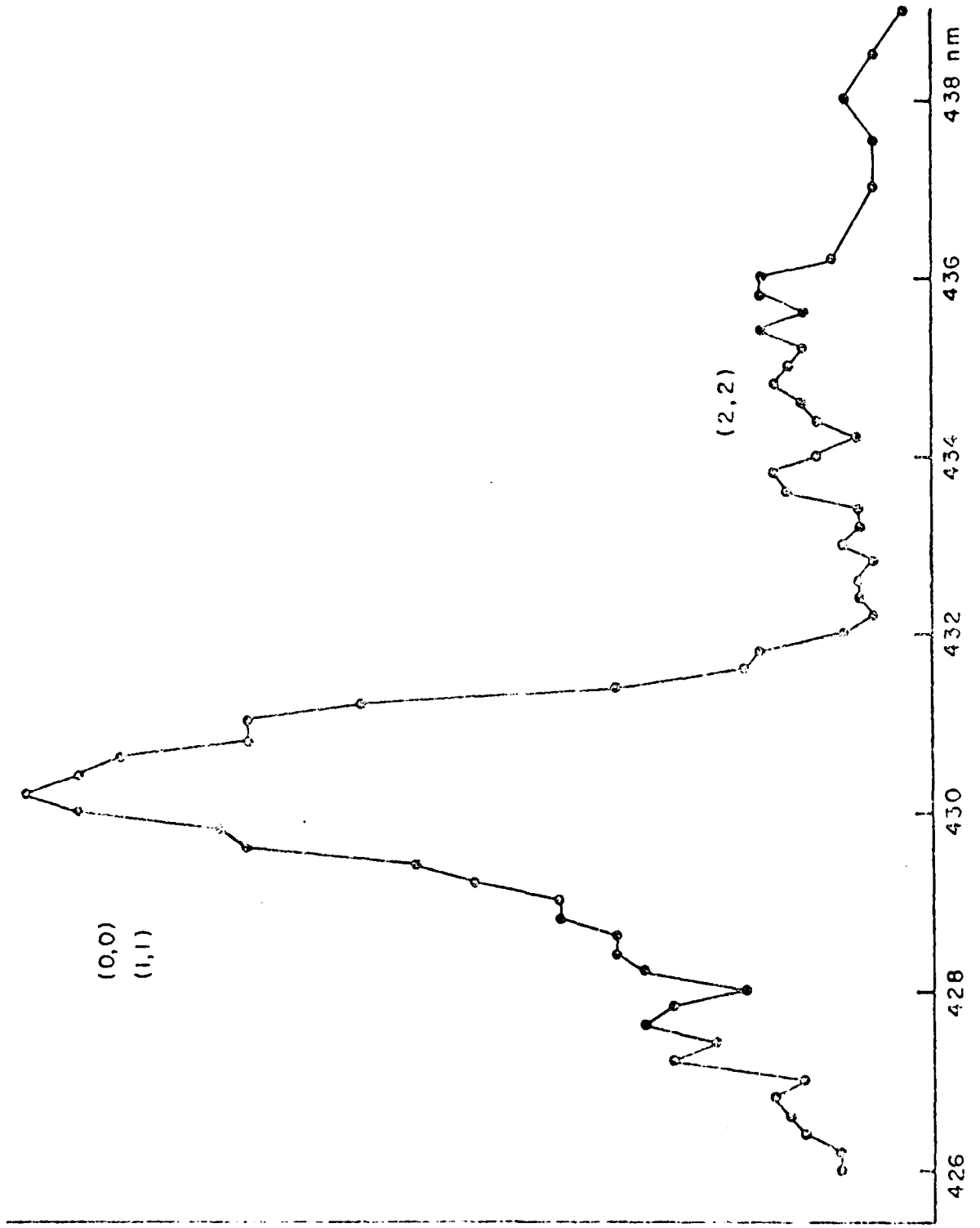
(0,0)
(1,1)
(2,2)
426
428
430
432
434
436
438 nm
EMISSION INTENSITY (arb units)

FIG. 1

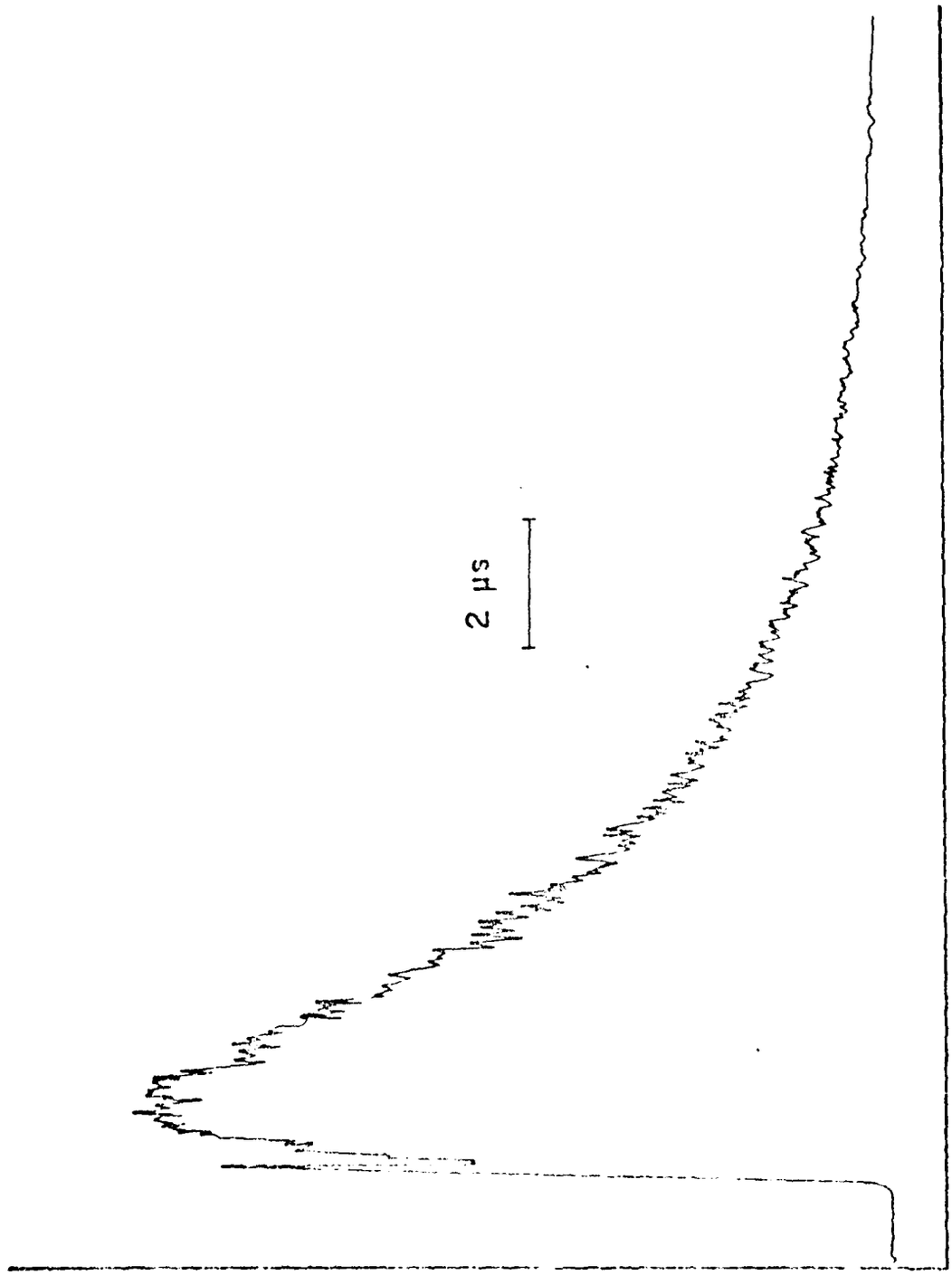

FIG. 2

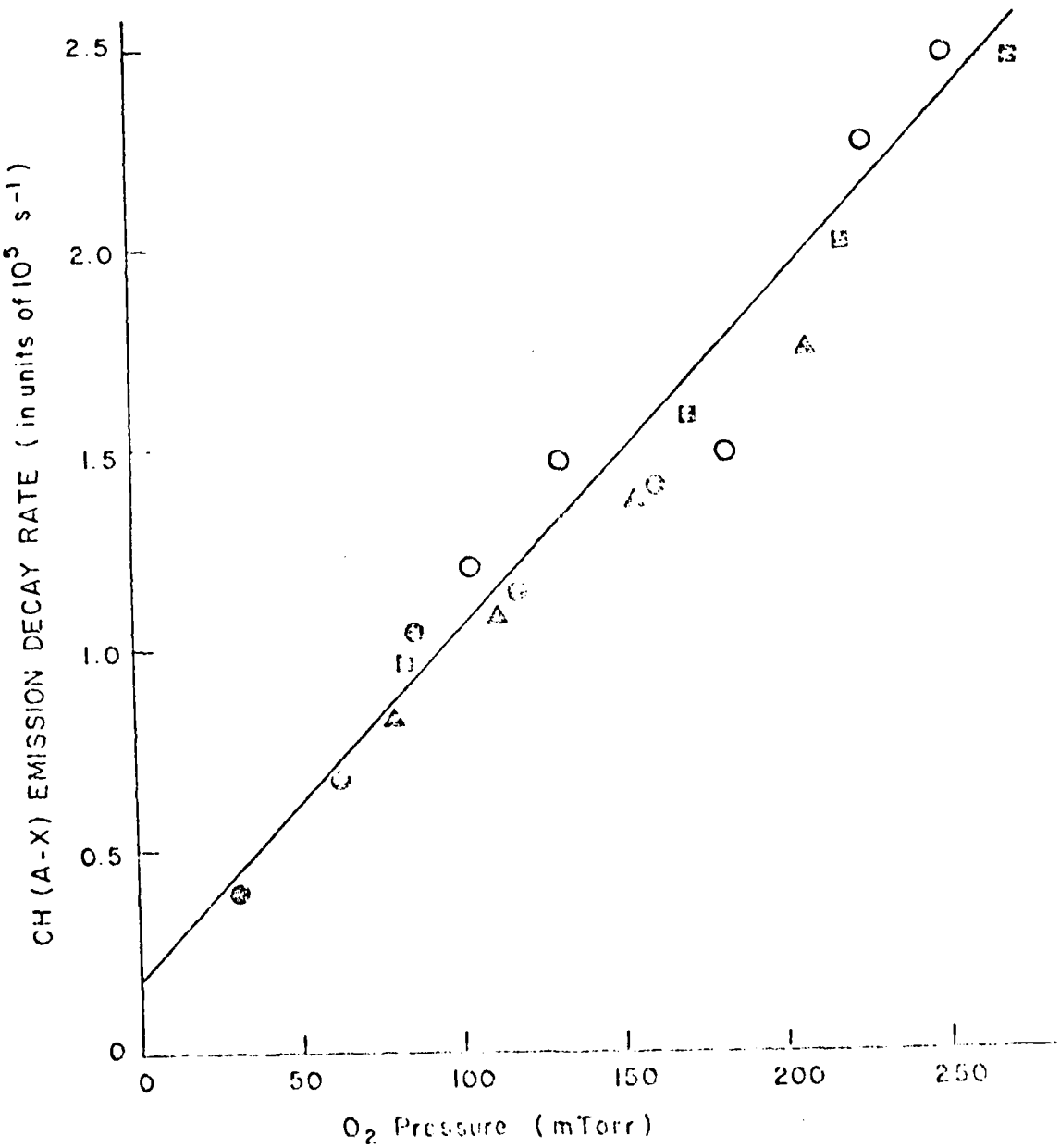
2.5
2.0
1.5
1.0
0.5
0
CH (A-X) EMISSION DECAY RATE (in units of 10^5 s^{-1})
0
50
100
150
200
250
O_2 Pressure (mTorr)

FIG. 3

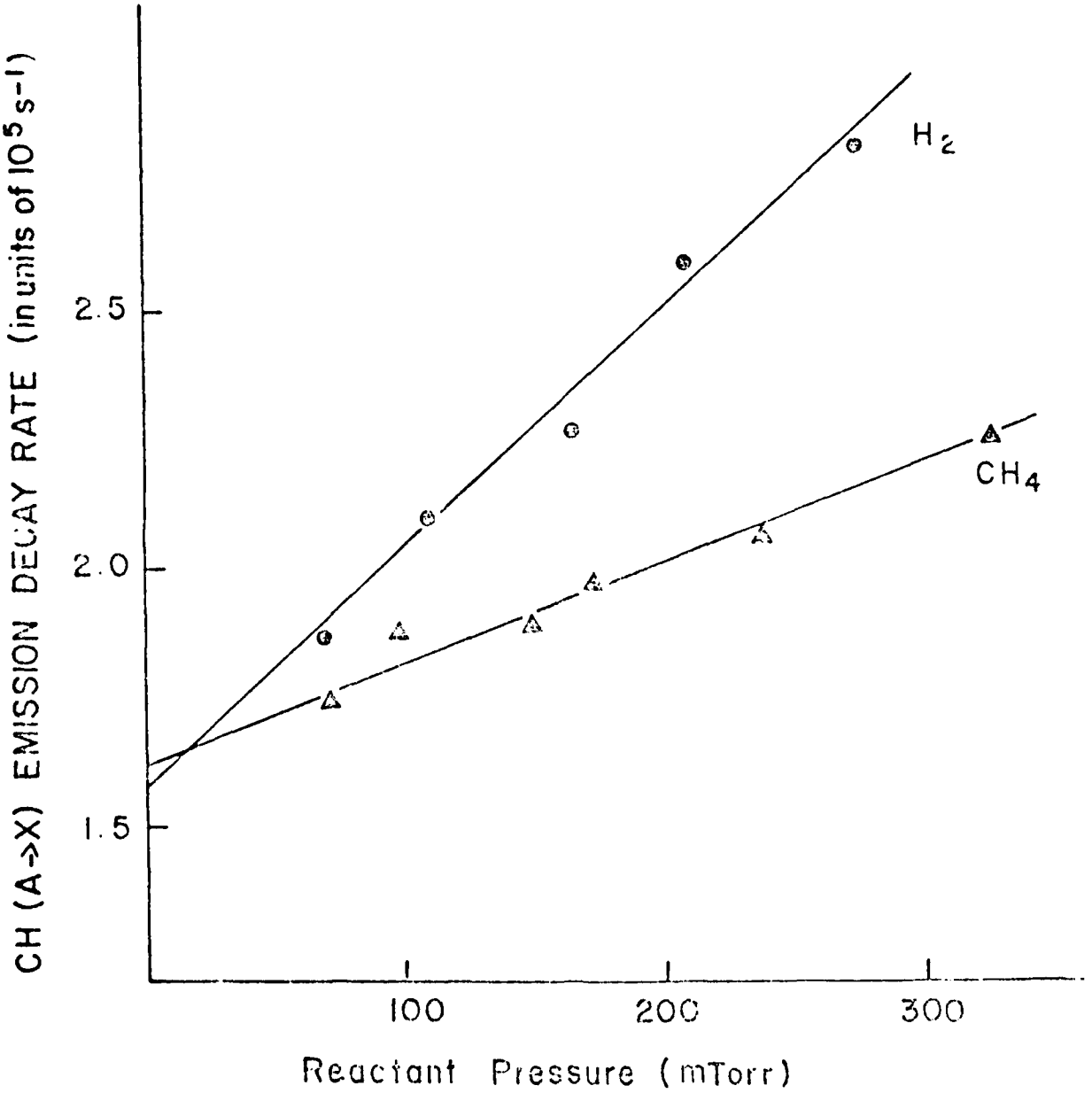
CH (A->X) EMISSION DECAY RATE (in units of $10^5 s^{-1}$)
2.5
2.0
1.5
100
200
300
Reactant Pressure (mTorr)
H_2
CH_4

FIG. 4